Modeling and Speed Tuning of a PMSM with Presence of Fissure Using Dragonfly Algorithm

Omar Aguilar-Mejía ¹, Abraham Manilla-García ², Ivan Rivas-Cambero ³ and Hertwin Minor-Popocatl ¹,*

¹ School Engineering, UPAEP University, Puebla 72410, Puebla, Mexico; omar.aguilar@upaep.mx
² Engineering Sciences, Pontificia Universidad Católica Madre y Maestra PUCMM, Santo Domingo 2748, Dominican Republic; a.manilla@ce.pucmm.edu.do
³ Faculty of Engineering, Universidad Politécnica de Tulancingo, Tulancingo de Bravo 43629, Hidalgo, Mexico; ivan.rivas@upt.edu.mx
* Correspondence: hertwin.minor@upaep.mx; Tel.: +52-222-229-94-00 (ext. 7431)

check for updates

Abstract: This paper presents a robust trajectory tracking control for a Permanent Magnet Synchronous Motor (PMSM) with consideration a fault, parametric uncertainties and external disturbances by effectively integrating robust optimal linear quadratic control. One kind of fault is considered in the machine, particularly the presence of fissure rotor. The dynamic model of the PMSM with the presence of fissure presents highly non-linear behaviors, which means that tuning is quite complicated, which the tuning was chosen through swarm intelligence optimization (Dragonfly Algorithm). A sensitivity analysis is carried out, in order to limit the search range to minimize the evaluation time. This methodology was used to diminish these defects during motor operation. Simulation results show that the optimal linear quadratic control method has a robust fault-tolerant performance.

Keywords: modeling of the continuous system; parameter estimation; modeling uncertainty; computational optimization method; inertia degradation; fissure mechanism; sensitivity

1. Introduction

The Permanent Magnet Synchronous Motors (PMSM), in addition to providing high performance in applications where it is necessary to correct the power factor, provide high torque and constant speed under variable loads, which makes them increasingly studied and used in applications that, until a few years ago, were restricted to induction motors [1]. One of the failures that causes more interest, especially in electric motors of considerable sizes, is due to vibratory problems, caused by imbalance, which, in turn, are generated by degradation in the rotor shaft, that is, fatigue phenomena which, finally, causes fracture in the rotor shaft [2]. The behavior of the propagation of fissures in solid materials is a subject of great interest in the field of engineering, thereby helping to preserve the life of mechanical devices [3]. A contribution to the fault-monitoring approach and input–output feedback linearization control of the induction motor (IM) in the closed-loop drive is presented in [4]. Two kinds of faults are considered in the machine, particularly the broken rotor bars and stator inter-turn short circuit faults. Therefore, the neural network (NN) technique is applied in order to identify the faults and distinguish them. However, the NN requires a relevant database to achieve satisfactory results. Hence, the stator current analysis based on the HFFT combination of the Hilbert transform and fast Fourier transform is applied to extract the amplitude of the harmonics and used them as an input dataset for NN.

Rotor faults have drawn more attention from the Artificial Intelligent (AI) research community in terms of utilizing fault-specific characteristics in its feature engineering. In [5], a review and definition

of the role of AI in rotors fault diagnosis (RFD) is provided, and an all-encompassing review of rotor faults is presented. That study is focused on (i) emphasizing the use of fault-specific characteristic features with AI, (ii) fault-wise analysis rather than component-wise analysis with appropriate fault categorization, and (iii) portraying the current research and analysis in accordance with different phases of an AI-based RFD framework.

The Active Magnetic Bearing (AMB) system will lose magnetic force if the power fails, which may cause fatal damage to the rotor and the back-up bearings. In order to improve the reliability of the AMB system, a power failure compensation control (PFCC) method is proposed in [6]. The power fails, the motor works as a generator and the back electromotive force (back EMF) is rectified by the anti-parallel diodes of the inverter. Meanwhile, a buck converter is utilized to convert the voltage from the DC-link of the inverter to the supply voltage for the AMB system. Similarly, in [7] a methodology for the detection of electrical and mechanical failures is presented using wavelets and the support of vector machines. Considering that some data are not available, for that methodology radial and tangential vibrations are required, as well as three-phase stator currents for different types of faults. For fault detection, they use identical speeds and loads with a number of mother wavelets; in the tests they did, the best result was obtained with the Shannon wavelet diagnosis and, notably, they were robust for all working conditions. Low cycle fatigue life for rotor systems driven by synchronous motors is predicted using the complex modal reduction technique in [8]. The system torsional model is derived using the lumping technique where, for accuracy, a large number of stations is considered. The effect of bearing viscous damping is accounted for in the equations of motion. The procedure is applied to an actual 19,000 hp synchronous motor driving a high-speed compressor. Simulation results showed excellent agreement in predicting the transient stresses between the full model and the two-modes reduced model with a vast reduction in computational time, i.e., around 90%. Moreover, the predicted fatigue life in terms of number of startups shows excellent agreement, with a maximum error of about 4.2% in the predicted life.

The advantages of permanent magnet synchronous motors are listed in [9], however, the un-modeled dynamics, the eventual mistakes and the strong nonlinearity diminish the motor performance quality. Indeed, since its synthesis is based on heuristic knowledge, linguistic description to perform a task and does not require a system model, the fuzzy logic control (FLC) idea is successfully applied to motor systems. The authors mentioned that the occurrence of failure may dramatically degrade the system performance and may even result in catastrophic system collapse. Therefore, in order to overcome this, they have designed a new fault tolerant control (FTC)-structure-based FLC to improve PMSM drive currents and speed controls during healthy and faulty conditions.

The dynamic model of electromechanical systems with the presence of degradation in the proposed inertia presents highly non-linear behaviors, which means that tuning is relatively complicated for the characteristic parameters, which are tuned using a population-based optimization algorithm, Fuzzy Control, and spectral tools [7–10]. In [11], the parameters of the 3-DOF PID controller are optimized by using the dragonfly algorithm (DA) for enhancing the system dynamics of a hybrid energy distributed power system subject to load and wind power variations. The algorithm is inspired from the static and dynamic swarming behavior of dragonflies, where the operation of DA is only dependent on the population size and the maximum iteration count. In [12], the DA was used to tune the controller parameters of the two-degrees-of-freedom PID for a multi-area power system. The performance of DA was evaluated in terms of tie-line power of control areas in the power system and the settling time of the deviations in frequency.

The main contribution of the paper is the design of a control scheme for a PMSM with the presence of fissure in the rotor shaft, causing this and, according to the fracture dynamics, degradation as well. In this work, a detailed analysis is provided of the modeling and tuning of this nonlinear dynamic system, which contributes to a more accurate theory of the dynamic behavior of the PMSM. The proposed algorithm combines a linear PID controller and an optimal quadratic controller to regulate the velocity trajectory tracking. To define the convergence domain of the possible regulation

gains in the dynamic model of the PMSM using the optimization dragonfly algorithm (DA) technique, a sensitivity analysis of the same is carried out, in order to limit the definition domain, minimize the evaluation time and help the convergence of the dynamic system. The control scheme of the PMSM is simple and robust and can operate within a very wide speed range.

The rest of the document is organized as follows: Section 2 develops the dynamic model of PMSM with the presence of a rotor fissure. In Section 3, a presentation of the control scheme of the dynamic PMSM model is given. In Section 4, the control tuning procedure through the Dragonfly algorithm is presented. Section 5 describes the procedure for conducting a sensitivity analysis. In Section 6, the simulation of the dynamic system of the PMSM is carried out. Finally, Sections 7 and 8 present the results of the implementation and a discussion of the results, respectively.

2. Dynamic PMSM Model with Presence of Rotor Fissure

Considering the voltage balance equations, the dynamic model of the PMSM in the reference system dq is obtained in a similar way to the modeling of a synchronous machine with field winding. To obtain the PMSM model, the flow links equations are eliminated and currents are defined as equal to zero by damping windings. Replacing the field current with a constant parameter due to the permanent magnet flow link, the model obtained is characterized by [13].

$$\frac{di_d}{dt} = \frac{V_d}{L_d} - \frac{r_s}{L_d}i_d + \frac{L_q}{L_d}\omega_r i_q \tag{1}$$

$$\frac{di_q}{dt} = \frac{V_q}{L_q} - \frac{r_s}{L_q}i_q + \frac{L_d}{L_q}\omega_r i_q - \frac{\lambda_m}{L_q}\omega_r \tag{2}$$

The dynamics of the PMSM rotor regarding angular velocity and angular position is defined by

$$\frac{d\theta}{dt} = \omega_r \tag{3}$$

$$\frac{d\omega_r}{dt} = \frac{P}{2J}[T_e - T_L - \beta\omega_r] \tag{4}$$

where

$$T_e = \frac{P}{2}\left[\frac{3}{2}\left(L_d - L_q\right)i_d i_q + \frac{3}{2}\lambda_m i_q\right] \tag{5}$$

2.1. Fracture Dynamics in the Rotor Shaft

The fissure behavior of the rotor shaft is proposed as a result of the variation in the stress on it, caused by the external load. The rotational effects of the rotor shaft generate a dynamic of opening and closing the fissure, which will generate, through work cycles, fatigue fracture that has a behavior similar to the fragile fracture. The fissure behavior takes the structure of the Paris equation, as in [14,15].

$$\frac{da}{dt} = cf\Delta k^n \tag{6}$$

The stress intensity factor is defined as

$$\Delta K = \Delta\tau_{max}\sqrt{\pi a} \tag{7}$$

From the expression defined by (7), the variation in torsional stress is proposed based on the behavior of a hollow circular section, which will increase in size due to degradation dynamics, starting from the concentration point of effort, where the presence of the fissure exists [16,17].

$$\Delta\tau_{max} = \frac{16(T_e - T_L)D}{\pi(D^4 - d^4)} \tag{8}$$

The smaller diameter of the rotor shaft d is proposed from the variation in the crack size, ($d = ga$), where g takes the breathing behavior of the axis proposed by Mayes and Davis, and can be defined as [18]

$$g = \frac{l + \cos(\omega_r t)}{2} \tag{9}$$

because of the presence of the fissure in the rotor shaft, the degradation in the rotational inertia of the rotor shaft has an effect proposed as

$$J_t = \frac{1}{8} m_s \left(D^4 - d^4 \right) \tag{10}$$

2.2. Dynamic Coupled Model

The dynamic study model with the presence of degradation in the rotational inertia of the rotor shaft can be formulated as

$$\frac{di_d}{dt} = \frac{V_d}{L_d} - \frac{r_s}{L_d} i_d + \frac{L_q}{L_d} \omega_r i_q \tag{11}$$

$$\frac{di_q}{dt} = \frac{V_q}{L_q} - \frac{r_s}{L_q} i_q + \frac{L_d}{L_q} \omega_r i_q - \frac{\lambda_m}{L_q} \omega_r \tag{12}$$

$$\frac{d\theta}{dt} = \omega_r \tag{13}$$

$$\frac{d\omega_r}{dt} = \frac{4P}{m_s \left\{ D^4 - [ga]^4 \right\}} \{ T_e - T_1 - \beta \omega_r \} \tag{14}$$

$$\frac{da}{dt} = cf\Delta k^n \tag{15}$$

3. Reference Model

The control scheme of the dynamic model of the PMSM with the characteristics defined by Equations (1)–(5) is carried out based on its linearization, without the presence of fissures, at the single point of global stable equilibrium of the dynamic system, defined as [19]

$$X_0 = \begin{bmatrix} i_{d0} & i_{q0} & \omega_{r0} \end{bmatrix}^T = \begin{bmatrix} 0 & 0 & 0 \end{bmatrix}^T \tag{16}$$

The first-order linear differential equations for the PMSM under which the simulation will be carried out, and, subsequently the development of the linear quadratic speed regulator, are

$$\frac{di_d}{dt} = -\frac{r_s}{L_d} i_d \tag{17}$$

$$\frac{di_q}{dt} = -\frac{r_s}{L_d} i_d - \frac{\lambda_m}{L_q} \omega_r \tag{18}$$

$$\frac{d\omega_r}{dt} = \frac{3P^2 \lambda_m}{8J} i_q \tag{19}$$

3.1. Desired Behavior of the Error

The error behavior regarding the change in speed between the desired angular speed and the rotor speed delivered by the PMSM is established as [20]

$$e_{\omega r} = \omega_{rd} - \omega_r \tag{20}$$

It is thought that the angular velocity error decreases exponentially in a limited time, which implies the relationship

$$e_{\omega r} = exp(-c_{\omega r}t) \tag{21}$$

The behavior of the current i_{qd} desired for the system based on the angular velocity error ω_r takes the form

$$i_{qd} = \frac{2J}{1.5P^2\lambda_m}\left[c_{\omega r}e_{\omega r}|\dot{\omega}_{rd}|\frac{PT_l}{2J_t}\right] \tag{22}$$

The load torque can be controlled directly by the current component of the axis q, therefore, the angular speed of the rotor can be controlled by the change in the current of the axis q, whereby the change in the current of the axis d is established at zero ($i_{dd} = 0$) to minimize current and resistance losses [21].

3.2. Optimal Linear Quadratic Control for States ω_r, i_q

For the control of the PMSM, the feedback of the states ω_r, i_q from the defined linear reference model is proposed, where the optimal gains are determined from the energy function E_Q as in [22]

$$E_Q = \int_0^\infty \left(X{\cdot}QX{\cdot}U_q{\cdot}RU_q\right)dt \tag{23}$$

The positive Hermitian matrices Q, R are defined as

$$Q = \begin{bmatrix} 100 & 0 \\ 0 & 1 \end{bmatrix}, \ R = [1] \tag{24}$$

The vector X takes the form

$$X = \begin{bmatrix} i_q & \omega_r \end{bmatrix}^T \tag{25}$$

The control function U_q takes the structure

$$U_q = -\begin{bmatrix} k_1 & k_2 \end{bmatrix}\begin{bmatrix} i_q \\ \omega_r \end{bmatrix} \tag{26}$$

The linearized system, for the variables i_q and ω_r under the action of the control, takes the form

$$\begin{bmatrix} i_q \\ \omega_r \end{bmatrix} = \begin{bmatrix} -\frac{r_s}{L_q} & -\frac{\lambda_m}{L_q} \\ \frac{3P^2\lambda_m}{8J} & 0 \end{bmatrix}\begin{bmatrix} i_q \\ \omega_r \end{bmatrix} + \begin{bmatrix} \frac{1}{L_q} \\ 0 \end{bmatrix}U_q \tag{27}$$

3.3. PID Controller for i_d Current

The structure of the proposed PID controller takes the form [23]

$$U_d = k_p\left[e_{id} + \frac{1}{k_i}\int e_{id}dt + k_d\frac{d}{dt}e_{id}\right] \tag{28}$$

To regulate the current i_d, it is based on the form of the decoupled linear equation defined in (17); when defining the control action, it is established as

$$\frac{di_d}{dt} = U_d - \frac{r_s}{L_d}i_d \tag{29}$$

The block diagram for regulating the PMSM i_d is shown in Figure 1.
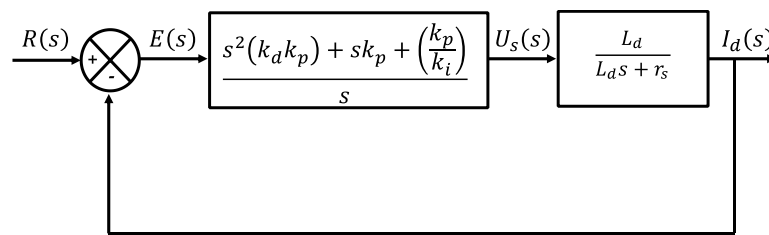
Figure 1. Block diagram, PID controller and plant.

Using the geometric place of the roots, the controller gains $\left(k_i, k_p, k_d\right)$ are calculated as

$$k_p = \frac{\alpha_1 + r_s}{L_d} \tag{30}$$

$$k_i = \frac{L_d k_p}{\alpha_2} \tag{31}$$

$$k_d = \frac{1 - L_d}{k_p L_d} \tag{32}$$

4. Tuning of Controller Using the Dragonfly Algorithms

The inspiration for the DA [24] is taken from the social behavior of the dragonflies when hunting their food (static swarm) and when they migrate (dynamic swarm). Considering these two behaviors, there are five factors involved in determining the individual dragonfly position: (a) separation; (b) alignment motion; (c) cohesion motion; (d) food Attraction; (e) predator distraction. There are two ways of updating the individual dragonfly position depending on the neighborhood position. If there is no dragonfly in the neighborhood radius, the individual position is updated considering the Levy flight equation and given as follows

$$X_{t+1} = X_t + lévy(dn)X_t \tag{33}$$

where *dn* is the number of decision variables. The Lévy flight function is given by

$$lévy(dn) = 0.01 \frac{r_1 \rho}{|r_2|^{\frac{1}{\beta}}} \tag{34}$$

where r_1 and r_2 are two random numbers in $[0, 1]$; β is a constant and ρ is computed as

$$\rho = \left(\frac{\Gamma(1+\beta)sin\left(\frac{\pi\beta}{2}\right)}{\Gamma\left(\frac{1+\beta}{2}\right)\beta 2^{\left(\frac{\beta-1}{2}\right)}}\right)^{\frac{1}{\beta}} \tag{35}$$

where $\Gamma(x) = (x-1)!$. Otherwise, the new position is calculated as follows

$$X_{t+1} = X_t + \Delta X_{t+1} \tag{36}$$

where ΔX_{t+1} is the step vector and can be obtained as

$$\Delta X_{t+1} = (sS_i + aA_i + cC_i + fF_i + eE_i) + w\Delta X_t \tag{37}$$

where *s* shows the separation weight; *a* is the alignment weight; *c* is the cohesion weight; *f* is a food actor; *e* is the enemy factor; *w* is the inertia weight, S_i indicates the separation of the $i-$th individual, A_i is the alignment of $i-$th individual, C_i is the cohesion of the $i-$th individual, F_i is the food source of the $i-$th individual, E_i is the position of enemy of the $i-$th individual and *t* is the

iteration number. The optimization process of DA is further explained by the pseudo code below [25]. The optimization process of DA is further explained by the pseudo code below (Algorithm 1):

Algorithm 1 Dragonfly Algorithm

    Define population size (M)
    begin the iteration counter $t = 1$
    Initialize the population by generating X_i for $i = 1, 2, 3 \ldots M$
    Calculate the objective function values of all dragonflies
    Update the food and the predator's location
    while (the stop criterion is not satisfied) do
        for $i = 1 : M$
            Update neighborhood radius (or update *w, s, a, c, f,* and *e*)
            if a dragonfly has at least one neighborhood dragonfly
                Separation motion
                Alignment motion
                Cohesion motion
                Food attraction motion
                Predator distraction motion
            else
                Update position vector using the Lévy flight function
            end if
        end for i
        Sort the population/dragonflies from best to and find the current best
    end while

Therefore, in this work, the dragonfly algorithm is used to calculate the optimization of the speed controller gains for the PMSM with the presence of degradation.

5. Sensitivity Analysis

The proposed tuning algorithm, using the dragonfly algorithm, searches for gains and the subsequent simulation of them in a defined domain. In order to limit the search domain, a sensitivity analysis is proposed for the PMSM speed control system. The sensitivity analysis will determine the variations in each of the gains involved, defined as the k_j parameters [26], where

$$k_j = \begin{bmatrix} k_1 & k_2 & k_i & k_p & k_d \end{bmatrix} \tag{38}$$

In addition, the study aims to ensure that this domain is optimal in terms of the consumption of the runtime of the algorithm. An energy function is defined, which aims to analyze the sensitivity of the PMSM model, defined as

$$E_T = E_C + E_P \tag{39}$$

where E_T is the total energy, E_C is the kinetic energy and E_P potential energy. The previous two energy functions can be defined as follows [1]

$$E_C = \int T_e \omega_r dt \tag{40}$$

$$E_P = \frac{1}{2}\left[\frac{i_d^2}{L_d} + \frac{i_q^2}{L_q} + \frac{P}{2J}\omega_r^2 \right] \tag{41}$$

The total energy is calculated using (1) and (2)

$$E_T = \int T_e \omega_r dt + \frac{1}{2}\left[\frac{i_d^2}{L_d} + \frac{i_q^2}{L_q} + \frac{P}{2J}\omega_r^2 \right] \tag{42}$$

Equation (42) can be expressed as a differential equation as

$$\frac{dE_T}{dt} = T_e \omega_r dt + \left[\frac{i_d}{L_d} \left(\frac{di_d}{dt} \right) + \frac{i_q}{L_q} \left(\frac{di_q}{dt} \right) + \frac{P\omega_r}{2J} \left(\frac{d\omega_r}{dt} \right) \right] \tag{43}$$

The energy cost function G, for the temporary evaluation period, can be defined as

$$G = \int E_T dt \tag{44}$$

The speed of change in the cost function in differential form, in the analysis time interval, can be described as

$$\frac{dG}{dt} = E_T \tag{45}$$

The set of differential equations that determines the behavior of the sensitivity of the parameters of the PMSM system is determined by combining the mathematical model of the machine and the energy cost function, and is expressed as

$$\frac{di_d}{dt} = \frac{V_d}{L_d} - \frac{r_s}{L_d} i_d + \frac{L_q}{L_d} \omega_r i_q \tag{46}$$

$$\frac{di_q}{dt} = \frac{V_q}{L_q} - \frac{r_s}{L_q} i_q + \frac{L_d}{L_q} \omega_r i_q - \frac{\lambda_m}{L_q} \omega_r \tag{47}$$

$$\frac{d\omega_r}{dt} = \frac{P}{2J} [T_e - T_1 - \beta \omega_r] \tag{48}$$

$$\frac{dE_T}{dt} = T_e \omega_r dt + \left[\frac{i_d}{L_d} \left(\frac{di_d}{dt} \right) + \frac{i_q}{L_q} \left(\frac{di_q}{dt} \right) + \frac{P\omega_r}{2J} \left(\frac{d\omega_r}{dt} \right) \right] \tag{49}$$

$$\frac{dG}{dt} = \int T_e \omega_r dt + \frac{1}{2} \left[\frac{i_d^2}{L_d} + \frac{i_q^2}{L_q} + \frac{P}{2J} \omega_r^2 \right] \tag{50}$$

From the system of Equations (46)–(50), the behavior of the cost function is obtained for the defined simulation time interval. The sensitivity of the system S_j, for each parameter of interest k_j, is as in

$$S_j = \frac{dG}{dk_j} \tag{51}$$

6. Simulation

The cost function to evaluate the performance of the dragonfly algorithm of profit search, considered as optimal, is that which minimizes the desired trajectories with those obtained in the interactions of the proposed system, which is defined from the state of interest ω_r as

$$c_j = [\omega_{rd} - \omega_r]^2 \tag{52}$$

To carry out the simulation of the dynamic PMSM system, the parameters and simulation coefficients are defined, Table 1 illustrates the numerical values that are taken into consideration during the model analysis.

The gains in the linear comparison system are determined from the linear analysis of speed regulation and take the following values

$$\begin{bmatrix} k_p \\ k_i \\ k_d \\ k_1 \\ k_2 \end{bmatrix} = \begin{bmatrix} -376.329 \\ 5.0 \\ 9.0 \\ 9990.09 \\ 930.0 \end{bmatrix}$$

Table 1. Simulation parameters for the PMSM model.

Parameters	Numerical Value	Units
L_d	6.73	Inductance [mH]
L_q	6.73	Inductance [mH]
r_s	2.6	Resistance [Ω]
J	3.5×10^{-5}	Rotational inertia [kgm^2]
m_s	0.1	Rotor mass [kg]
λ_m	0.319	Magnetic flux [Wb]
f	$188.5/2\pi$	Frequency [Hz]
β	5×10^{-5}	
c	10×10^{-11}	Proportional coefficient
n	3	Proportional exponent
D	0.137409	Root of rotor diameter [m$^{1/2}$]
T_L	5	Load torque
i_{d0}	0	Initial current d
i_{q0}	0	Initial current q
ω_{r0}	0	Initial angular velocity [rad/s]
θ_0	0	Initial angular position [rad]
a_0	3×10^{-8}	Initial fissure size [m]
V_s	90	Nominal Voltage [V]
c_{ω_r}	1500.5	
ω_{rd}	188.5	Desired angular velocity [rad/s]
α_1	-1	Desired Root 1
α_2	-1	Desired Root 2

The process of searching for the gains of the speed control scheme for the non-linear dynamic system of PMSM is presented in the diagram shown in Figure 2. The step of searching and testing the parameters of the controller is carried out by means of dragonfly algorithm.
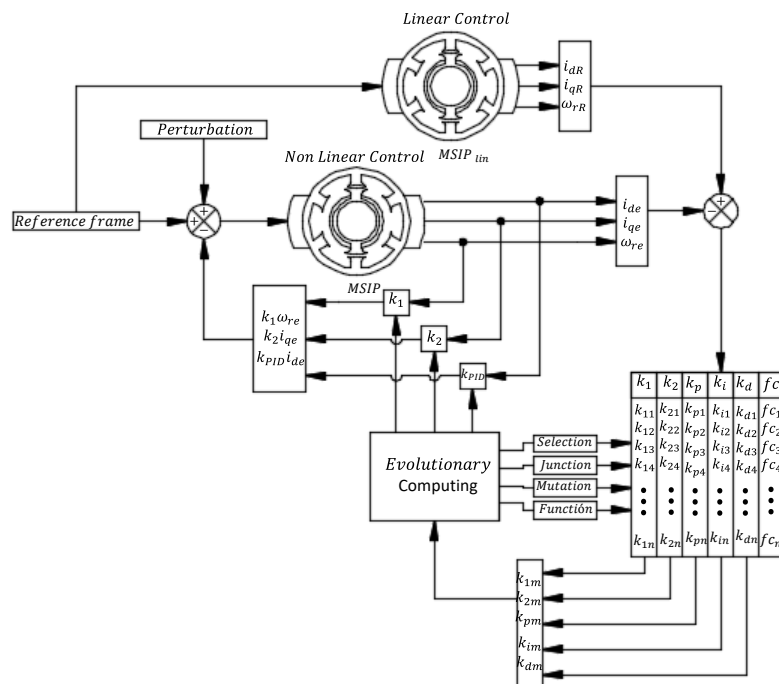
Figure 2. Diagram of the search process of the speed controller gains for the non-linear dynamic system of the PMSM.

7. Results

Using the proposed model of the PMSM with the presence of fissure in Section 3 and the linear comparison reference defined in Section 4, a convergence analysis is performed between both models subjected to the disturbance defined by the system of equation [27] as

$$
\begin{aligned}
V_d &= V_s \sqrt{2} sin(\delta)\\
V_q &= V_s \sqrt{2} cos(\delta)
\end{aligned}
\tag{53}
$$

The variation in the displacement angle of the rotor δ is determined from

$$
\frac{d\delta}{dt} = \omega_r - 2\pi f
\tag{54}
$$

In Figure 3 it can be seen that, under the disturbance given to both models of the PMSM under study, the simulation convergence time interval, for the i_d current, is less than 0.01 s; subsequently, the i_d current diverges in the reference linear and the nonlinear proposal. For the states i_q and ω_r, it is observed that the convergence is for the entire simulation time interval.
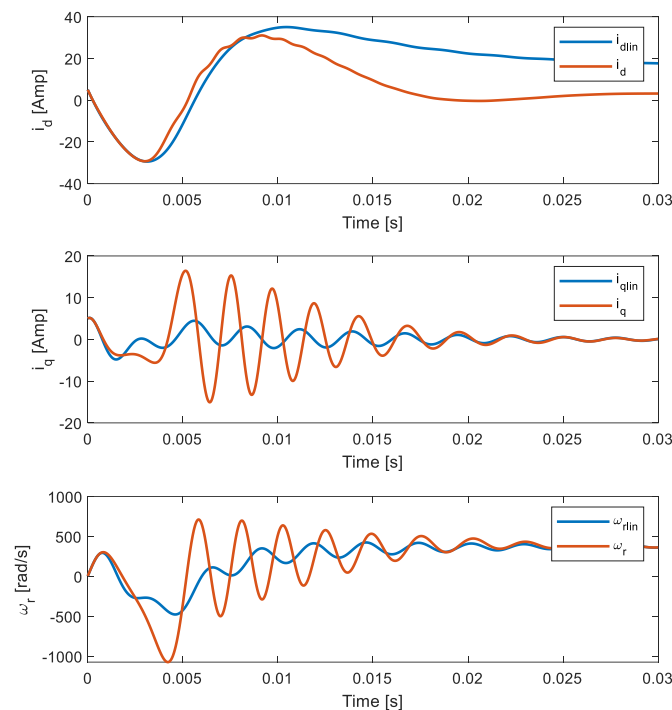
Figure 3. Variables of state of interest, current i_d (upper), current i_q (medium), angular velocity (lower) of the linear system and non-linear system.

From the comparison between the proposed model with the presence of degradation in rotational inertia and the linear model of the PMSM, it is observed that they only converge under a small region of time (0.01 s). This time interval is insufficient for a proper degradation analysis, where simulation times will be greater than 2000 s, and where the controller must show its efficiency to overcome the modeling limitations and ensure that the variables of interest converge to the desired reference values (angular velocity and current consumption).

The delimitation of the search domain of each of gains involved in controller action will help achieve this goal. Figures 4–8 show the behavior of the cost function proposed in the analysis of sensitivity for each of the gains involved.
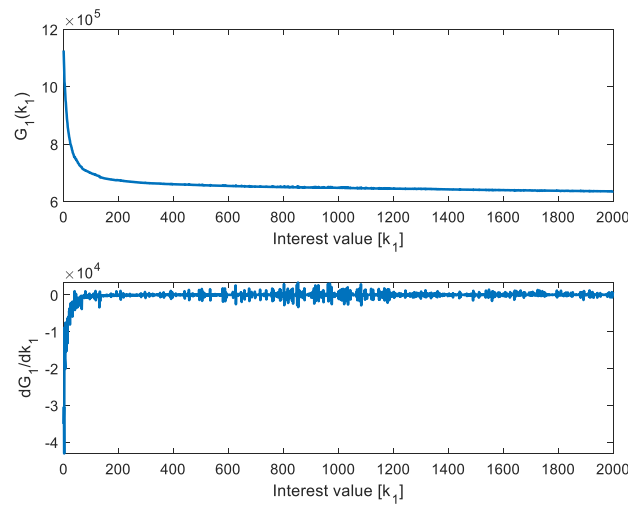
Figure 4. Energy rate (higher) and energy variation (lower) for the gain k_1.
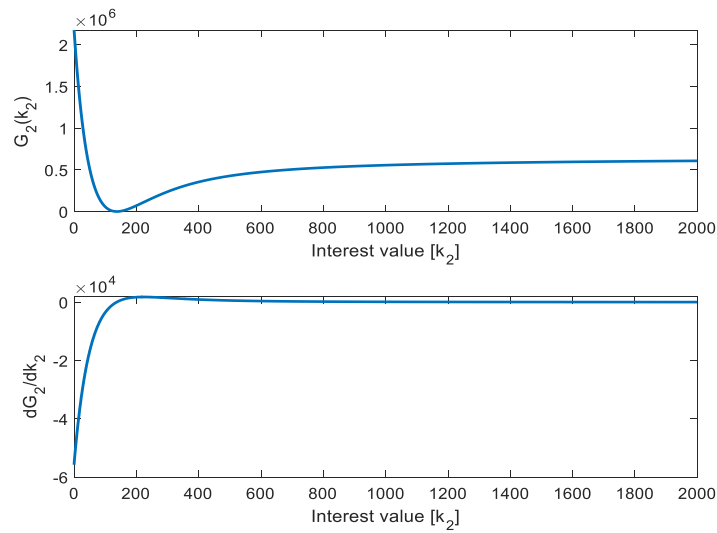
Figure 5. Energy rate (higher) and energy variation (lower) for the gain k_2.
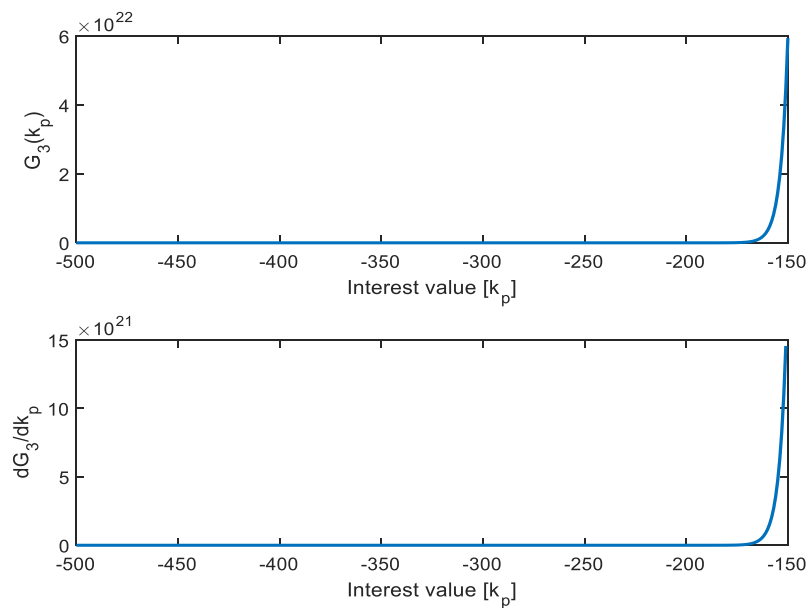
Figure 6. Energy rate (higher) and energy variation (lower) for the k_p gain.
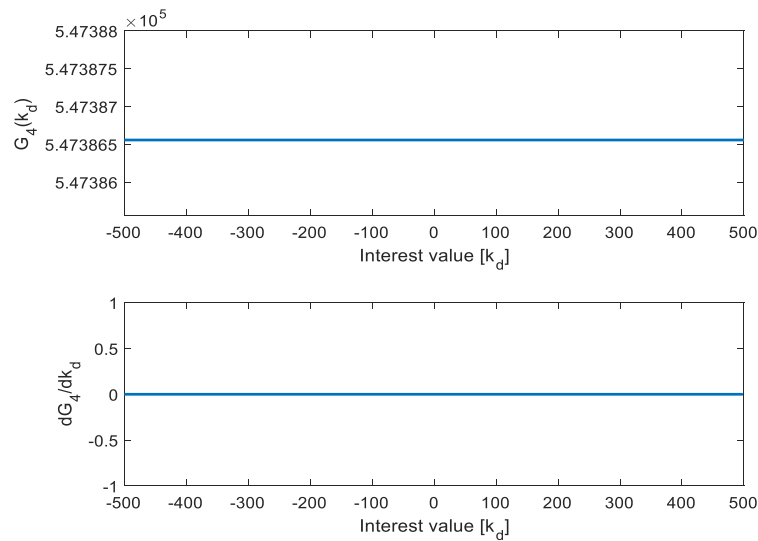
Figure 7. Energy rate (higher) and energy variation (lower) for the k_d gain.
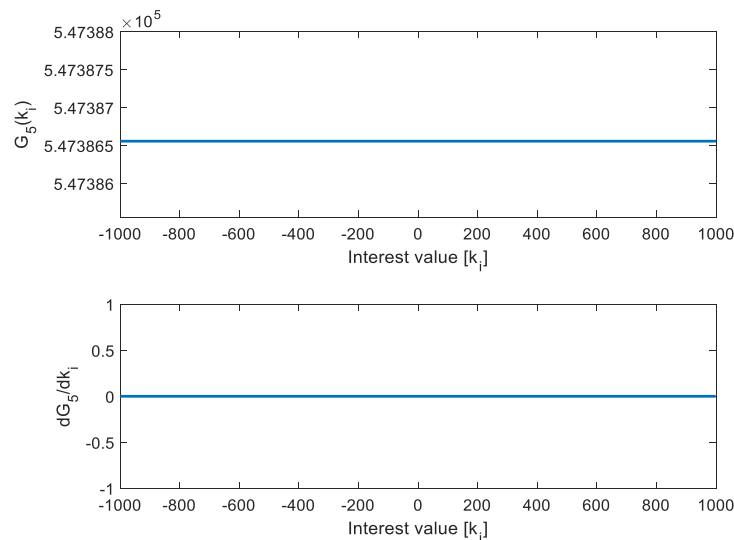
Figure 8. Energy rate (higher) and energy variation (lower) for the k_i gain.

It is observed that sensitivity of the dynamic system and the energy consumption are exponentially increased, with gains of k_1 less than 200. Similarly, the numerical instability of algorithm grows exponentially, achieving the non-convergence of the solution of the mathematical model, therefore, those values should be avoided. For the gain k_2, a concave behavior is observed in the range of values near to 120; where the minimum sensitivity point is located, energy consumption will be minor as well as the time of algorithm computation, therefore, an interval close to that value of sensitivity must be chosen.

It is observed that, within the most representative variations in energy consumption, there is the gain k_p, which is very sensitive to values greater than −185. Where the sensitivity is reflected in the energy consumption, which increases exponentially, the time of computation will be similar, increasing the numerical instability of the algorithm; therefore, these values should be avoided.

For the gains k_i and k_d the behavior of the sensitivity in the face of gain variation is indifferent, therefore, any interval chosen as the search function will not affect the time spent on computing resources. Using the previous sensitivity analysis, intervals of search for gains were chosen close to trajectories that minimize the proposed energy consumption, which are defined as

$$k_1 = \begin{bmatrix} 150, & 2000 \end{bmatrix}; k_2 = \begin{bmatrix} 120, & 500 \end{bmatrix}; k_p = \begin{bmatrix} -900, & -185 \end{bmatrix}; k_i = \begin{bmatrix} -10, & 10 \end{bmatrix}; k_d = \begin{bmatrix} 0.1, & 20 \end{bmatrix}$$

For the convergence test between answers to the control action of the linear test model and the proposed model of nonlinear PMSM, the desirable behavior of angular velocity is proposed through a defined step function where

$$\omega_{rd} = \begin{cases} 188.5 \frac{\text{rad}}{\text{s}} & if\ t < 0.0005\ \text{s} \\ 100.0 \frac{\text{rad}}{\text{s}} & if\ t > 0.0005\ \text{s} \end{cases}$$

The response of behavior of the angular velocity ω_r and current consumption corresponding to i_q of linear comparison model of the PMSM in the desired angular velocity input ω_{rd} are shown in Figure 9. The parameters for proper convergence of search-tuning of the DA after numerical simulation tests are shown in Table 2.
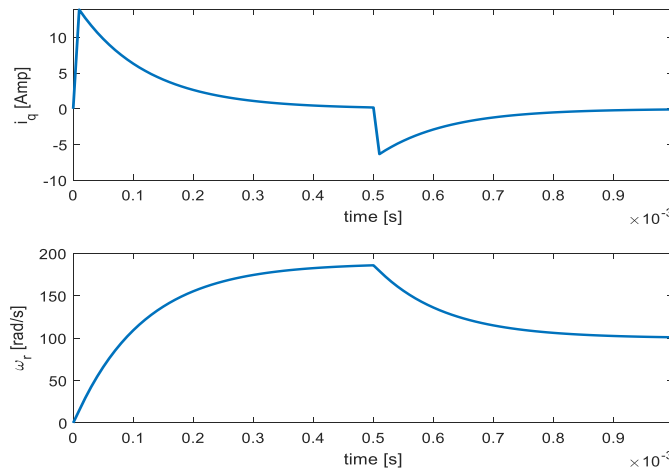
Figure 9. Desired behavior of angular velocity (lower) and current consumption i_q (higher) in the linear comparison system.

Table 2. Dragonfly algorithm implementation details.

Parameters	Numerical Value
Population size	40
Maximum of iteration	100
Random values	$r_1 = r_2 = [0; 1]$
Separation weight	0.12
Alignment weight	0.12
Cohesion weight	0.75
Food factor	1
Enemy factor	1
Inertia weight	0.9–0.2
β	1.5

In Figure 10, the behavior of the DA regarding the pursuit of gains for tune the PMSM model is illustrated, with the presence of degradation in rotational inertia, under search conditions defined by the sensitivity analysis and the desired model of behavior of linear PMSM, as well as angular speed's desired behavior under a first search iteration. Figures 10 and 11 show, in different colors, the dynamic response of the closed-loop system (controller-PMSM), with all gains calculated in the first iteration and in the tenth search evolution, respectively.
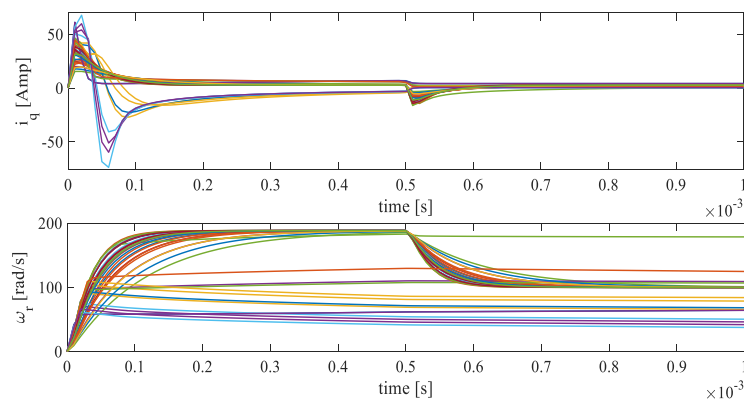
Figure 10. Behavior of the dragonfly algorithm in the search of tuning, for both current consumption (up), and desired angular velocity (below), first iteration.
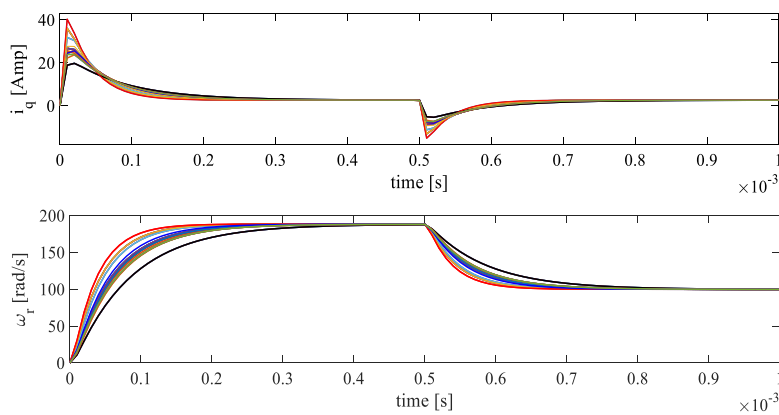
Figure 11. Behavior of the DA for the dynamic system PMSM with crack presence, better control gains in the tenth search evolution.

In Figure 11, the behavior of the collection of gains generated by the DA is illustrated, and applied to a proposed model of the PMSM with the presence of degradation in rotational inertia. In the tenth search evolution, the convergence of the behaviors of all these gains obtained by the DA is obtained for the desired model of linear reference to the PMSM. In Figure 12, the best response obtained in the ω_r angular velocity tuning process is illustrated. The consumption of current i_q by the controller action defined by the dragonfly algorithm, in the case of the analysis, is

$$k_1 = 1521.6; \ k_2 = 223.1; \ k_p = -799.4; \ k_i = -4.4; \ k_d = 12.4$$
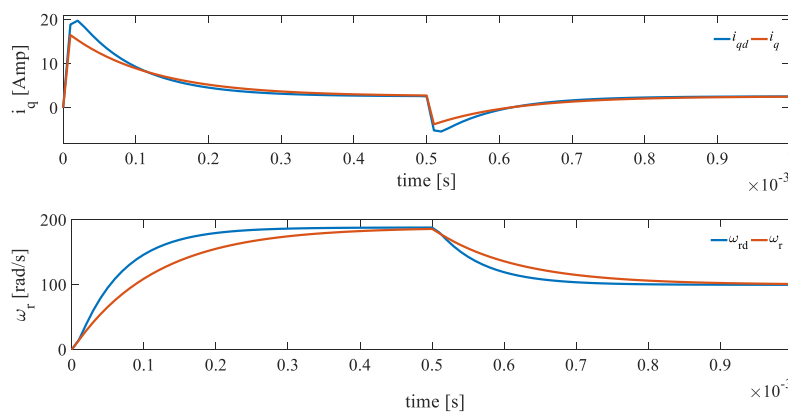
Figure 12. Behavior of the DA for the dynamic system of the PMSM with the presence of a crack, gains with the least error.

It is observed that the obtained trajectory has a performance with behavior close to the desired angular velocity, ω_{rd}, therefore, the gains obtained are considered optimal. The behavior of the proposed nonlinear model and linear model PMSM reference for times greater than 0.001 s is achieved with these gains, so the robustness of the tuning algorithm is checked under the presence of the initial fissure given. Figure 13 illustrates the ω_r angular velocity behavior and consumption of current i_q under the action of the gains obtained through the simulation done for an evaluation time of 0.03 s, which shows that the system keeps responding to the action of control.
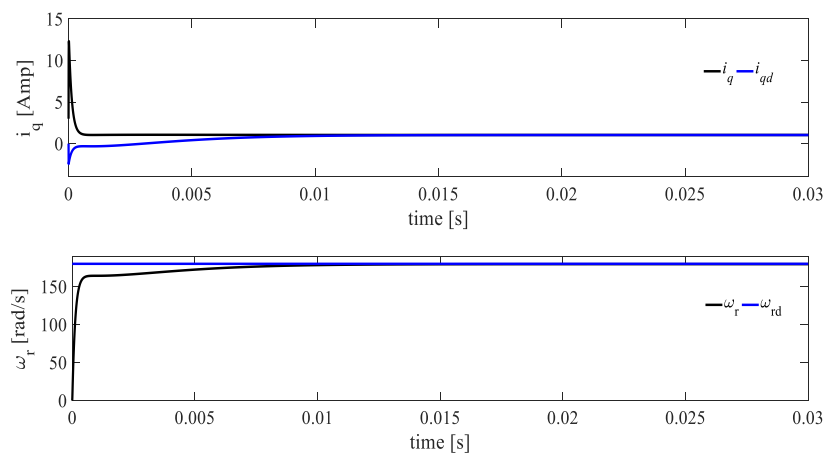
Figure 13. Comparison, best gains found, nonlinear system, linear system for times greater than the attractor of the equilibrium point.

In Figure 14, the speed behavior angular ω_r and current consumption i_q of the nonlinear model of the PMSM, proposed with degradation in rotational inertia for a simulation time of 450 s, are illustrated. The time of evaluation is large so that the effects of steady state be seen, and it is observed that the behavior of the desired angular velocity ω_{rd} is maintained under the action of control. For the given simulation, an angular velocity given by a Bézier polynomial ¥ is desired to provide a sufficiently smooth transfer between the actual and desired speed reference values, within a specific time interval. Then, the reference trajectory profile is as follows

$$
\omega_r^* = \begin{cases}
\omega_1 & for\ t \leq T_1 \\
\omega_1 ¥(t, T_1, T_2) & for\ T_1 < t \leq T_2 \\
\omega_1 & for\ T_2 < t \leq T_3 \\
\omega_2 - (\omega_2 - \omega_1)¥(t, T_3, T_2) & for\ T_3 < t \leq T_4 \\
\omega_2 & for\ T_4 < t \leq T_5 \\
\omega_3 + (\omega_3 - \omega_2)¥(t, T_5, T_6) & for\ T_5 < t \leq T_6 \\
\omega_3 & for\ T_6 < t \leq T_7 \\
\omega_4 + (\omega_4 - \omega_3)¥(t, T_7, T_8) & for\ T_7 < t \leq T_8
\end{cases}
\tag{55}
$$

where $\omega_1 = 0$ rpm, $\omega_2 = 800$ rpm, $\omega_3 = 1600$ rpm, $\omega_4 = 600$ rpm, $T_1 = 0$ s, $T_2 = 18$ s, $T_3 = 135$ s, $T_4 = 150$ s, $T_5 = 290$ s, $T_6 = 305$ s, $T_7 = 420$ s, $T_8 = 450$ s, and $Y =$ is the Bézier interpolation polynomial

$$
¥ = K^5 \left[r_1 - r_2 K + r_3 K^2 - r_4 K^3 + \ldots - r_6 K^5 \right]
\tag{56}
$$

$$
K = \frac{t + T_1}{T_2 - T_1},
\tag{57}
$$

with $r_1 = 252$, $r_2 = -1050$, $r_3 = 1800$, $r_4 = -1575$, $r_5 = 700$ and $r_6 = -126$.
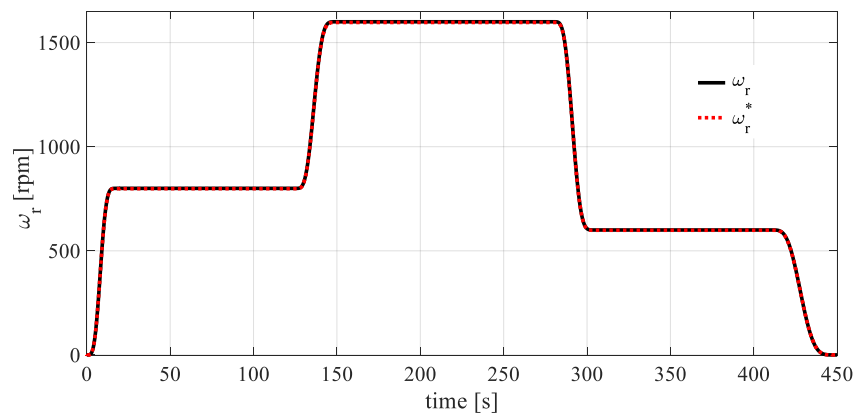
Figure 14. Behavior of the angular velocity of reference for the evaluation time $t = 450$ s.

The behavior of the fissure inside the PMSM is shown in Figure 15. It is observed that the fissure grows suddenly with the PMSM startup and, because of inertial effects, as the working time of the PMSM continues, the growth of the fissure is gradual and in an exponential form, which will exhibit a progressive degradation in the rotational inertia of the rotor shaft, thereby validating the proposed dynamic behavior. The tracking error for optimal linear state feedback controller is shown in Figure 16.
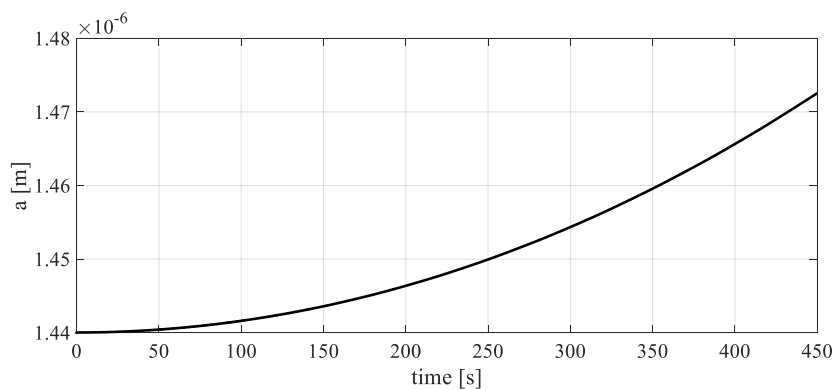
Figure 15. Fissure behavior of the dynamic model proposed in the PMSM rotor.
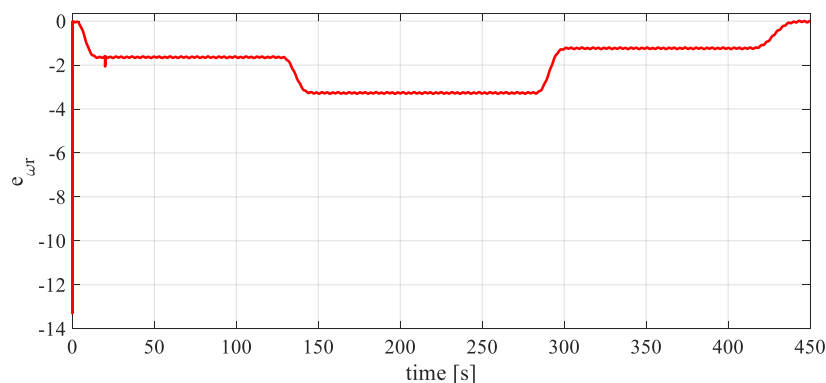
Figure 16. Speed tracking error for the evaluation time $t = 450$ s.

8. Conclusions

This paper presents an application of one metaheuristic (dragonfly algorithm) for tuning a PID, and optimal linear quadratic controllers for a PMSM with the presence of rotor fissure. The optimization procedure was employed considering simulation with the non-linear system model. This strategy contains the speed and current control loops. In order to define the search range for DA, a sensitivity

analysis of gains of the PMSM controller was carried out. The sensitivity analysis of gains of the PMSM controller with the presence of degradation in rotational inertia can find search intervals that help to minimize the tuning time of the DA. The dragonfly algorithms confirm the feasibility and effectiveness of the parameter optimization for the optimal linear quadratic and PID controller. The results of the simulation show that the controller has a good performance and fast tracking speed under presence of fissure in the rotor shaft and external perturbation. The controller aims to ensure speed tracking tasks while significantly reducing the speed overshoot. Note that there was no need to retune the controllers for different kinds of operations; therefore, the designed controller is convenient to be realized. This shows the advantages of advanced controller tuning. Since the controller exhibits an excellent performance, it is ideal for application in process industries.

The PMSM model with the rotational inertia degradation coupling in the shaft allows for applications in the field of preventive maintenance, failure control or determination of failure intervals of rotating machines, to name a few fields of application. It is observed that, under the given working conditions, the dynamic model of the PMSM with the presence of degradation in the rotational inertia of the rotor axis is adequately tuned to the requested references by means of the DA used for any analysis time. The proposed PMSM model with the presence of rotational inertia degradation is considered congruent with the expected degradation behavior typical of rotating machines: the size of the internal fissure continues to grow in an exponential form and gradual manner until the fracture finally occurs.

Nomenclature

The variables involved in the modeling of the PMSM with the presence of degradation in rotational inertia are defined in Table 1.

Definition of the variables involved in the PMSM model.

Parameters	Definition
i_d, i_q	Stator currents in the rotating dq reference frame
θ	Angular position of the rotor shaft
ω_r	Angular speed of the rotor
a	Fissure size
V_d, V_q	Stator voltages in the rotating dq reference frame
L_d, L_q	Stator inductances on the dq reference axes
r_s	Stator phase resistance
P	Number of pole pairs
J	Polar moment of inertia
m_s	Rotor mass
J_t	Rotational inertia dependent on fissure size
λ_m	Permanent magnetic flow
f	Fundamental rotor frequency
β	Viscous damping coefficient
c	Proportional coefficient (material dependent)
n	Proportional exponent (material dependent)
D	Root of rotor shaft diameter
T_L	External load torque

T_e	Electric torque (generated by the motor)
g	Mayes and Davis fissure respite function
d	Diameter of the hole in the rotor shaft due to the fissure
Δk	Variation of the stress concentrator
$\Delta \tau_{max}$	Torsional stress variation in the rotor shaft
i_{d0}, i_{q0}, ω_{r0}, θ_0, a_0	Initial model conditions
V_s	Nominal value of the voltage applied in phases *dq*
δ	Electric angular displacement
e_{ω_r}, e_{id}	System Status Errors
$c_{\omega r}$	Desired error coefficient
i_{qd}, i_{dd}, ω_{rd}	Desired values of system states
Q, R	Hermetic Matrices of optimal control
X	Vector of linear quadratic optimal control states
U_q, U_d	System control inputs
k_1, k_2	Linear Quadratic Optimal Control Gains
k_p, k_i, k_d	Gains from Proportional Integral and Derivative Control (PID)
α_1, α_2	PID Controller Profit Locating Roots
E_Q	Linear Quadratic Optimum Controller Power
E_T	Total energy of the PMSM dynamic system
E_C	PMSM kinetic energy
E_P	PMSM potential energy
G	Energy cost of the PMSM dynamic system
S_i	PMSM dynamic system sensitivity
c_j	Cost localization function of optimal earnings
k_j	Optimal earnings vector
ω_{rj}	Value obtained from the *j*th search for speed gain

References

1. Gieras, J.F.; Wing, M. *Permanent Magnet Motor Technology: Desing and Applications*, 2nd ed.; Marcel Dekker: New York, NY, USA, 2002; pp. 1–15a, 169–187b.
2. Quiroz, J.C.; Maurin, N.; Rezazadeh, M.; Izadi, M.; Misron, N. Fault detection of broken rotor bar in LS-PMSM using random forests. *Measurement* **2018**, *116*, 273–280. [CrossRef]
3. Bachschmid, N.; Pennacchi, P.; Tanzi, E. *Cracker Rotors*; Springer: Berlin, Germany, 2010; pp. 4–14.
4. Harzelli, I.; Menacer, A.; Ameid, T. A fault monitoring approach using model-based and neural network techniques applied to input–output feedback linearization control induction motor. *J. Ambient. Intell. Human. Comput.* **2020**, *11*, 2519–2538. [CrossRef]
5. Nath, A.G.; Udmale, S.S.; Singh, S.K. Role of artificial intelligence in rotor fault diagnosis: A comprehensive review. *Artif. Intell. Rev.* **2020**. [CrossRef]
6. Liu, G.; Mao, K. A Novel Power Failure Compensation Control Method for Active Magnetic Bearings Used in High-Speed Permanent Magnet Motor. *IEEE Trans. Power Electron.* **2016**, *31*, 4565–4575. [CrossRef]
7. Gangsar, P.; Tiwari, R. Diagnostics of mechanical and electrical faults in induction motors using wavelet-based features of vibration and current through support vector machine algorithms for various operating conditions. *J. Braz. Soc. Mech. Sci. Eng.* **2019**, *41*, 71. [CrossRef]
8. Al-Bedoor, B.O.; Moustafa, K.A.; Al-Hussain, K.M. Predicting the fatigue life of synchronous motor-driven compressor using the complex modal reduction technique. *Comput. Methods Appl. Mech. Eng.* **2000**, *187*, 53–68. [CrossRef]
9. Mekki, H.; Benzineb, O.; Boukhetala, D.; Chrifi-Alaoui, L.; Tadjine, M. Fault Tolerant Design for Permanent Magnet Synchronous Motor using Fuzzy Speed Controller. *IFAC-PapersOnLine* **2016**, *49*, 315–320. [CrossRef]
10. Villalobos-Piña, F.; Alvarez-Salas, R. Algoritmo robusto para el diagnóstico de fallas eléctricas en motor de inducción trifásico basado en herramientas espectrales y ondeletas. *Rev. Iberoam. Automática Inf. Ind.* **2015**, *12*, 292–303. [CrossRef]

11. Guha, D.; Roy, P.K.; Banerjee, S. Optimal tuning of 3 degree-of-freedom proportional-integral-derivative controller for hybrid distributed power system using dragonfly algorithm. *Comput. Electr. Eng.* **2018**, *72*, 137–153. [CrossRef]

12. Simhadri, K.; Mohanty, B.; Mohan, R. Optimized 2DOF PID for AGC of Multi-area Power System Using Dragonfly Algorithm. In *Applications of Artificial Intelligence Techniques in Engineering*; Malik, H., Srivastava, S., Sood, Y., Ahmad, A., Eds.; Springer: Singapore, 2019; pp. 11–22. [CrossRef]

13. Xue, W.; Li, Y.; Cang, S.; Jia, H.; Wang, Z. Chaotic behavior and circuit implementation of a fractional-order permanent magnet synchronous motor model. *J. Frankl. Inst.* **2015**, 2887–2898. [CrossRef]

14. Venkatesan, K.; Liu, Y. Subcycle fatigue crack growht formulation under positive and negative stress ratios. *Eng. Fract. Mech.* **2018**, *189*, 390–404. [CrossRef]

15. Andrade, A.A.; Mosquera, W.A.; Vanegas, L.V. Modelos de crecimiento de grietas por fatiga. *Entre Cienc. Ing.* **2015**, *9*, 39–48. [CrossRef]

16. Arana, J.L.; González, J.J. *Mecánica de la Fractura*; Servicio Editorial de la Universidad del País Vasco: Leioa, Spain, 2011; p. 186.

17. Barter, S.; White, P.; Burchill, M. Fatigue Crack path manipulation for crack growth rate measurement. *Eng. Fract. Mech.* **2016**, *167*, 224–238. [CrossRef]

18. Genta, G. *Dynamics of Rotating System*; Springer: Berlin, Germany, 2005; pp. 332–354.

19. Rasoolzadeh, A.; Tavazoei, M.S. Prediction of chaos in non-salient permanentmagnet synchronous machines. *Phys. Lett. A* **2012**, 73–79. [CrossRef]

20. Krishnan, R. *Permanent Magnet Synchronous and Brushless DC Motor Drives*; CRC Press: Boca Raton, FL, USA, 2010; pp. 225–276.

21. Aguilar-Mejía, O.; Tapia–Olvera, R.; Valderrabano-González, A.; Rivas-Cambero, I. Adaptive neural network control of chaos in permanent magnet synchronous motor, Taylor and Francis Group. *Intell. Autom. Soft Comput.* **2015**, *22*, 499–507. [CrossRef]

22. Xu, W.J. Permanent Magnet Synchronous Motor with Linear Quadratic Speed Controller. *Energy Procedia* **2011**, *14*, 364–369. [CrossRef]

23. Yun-Jie, W.; Guo-Fei, L. Adaptive disturbance compensation finite control set optimal control for PMSM systems based on sliding mode extended state observer. *Mech. Syst. Signal. Process.* **2018**, *98*, 402–414. [CrossRef]

24. Meraihi, Y.; Ramdane-Cherif, A.; Acheli, D.; Mahseur, M. Dragonfly algorithm: A comprehensive review and applications. *Neural Comput. Appl.* **2020**, *32*, 16625–16646. [CrossRef]

25. Mirjalili, S. Dragonfly algorithm: A new meta-heuristic optimization technique for solving single-objective, discrete, and multi-objective problems. *Neural Comput. Appl.* **2016**, *27*, 1053–1073. [CrossRef]

26. Boroni, G.; Lotito, P.; Clausse, A. Análisis de sensibilidad de sistemas algebraicos diferenciales. *Asoc. Argent. Mecánica Comput.* **2006**, *25*, 1071–1085.

27. Krauze, P.; Wasynczuk, O.; Sudhoff, S.; Pekarek, S. *Analysis of Electric Machinery and Drive Systems*, 3rd ed.; IEEE Press: Hoboken, NJ, USA, 2013; pp. 191–256.